Theoretical studies on kinetics, mechanism and thermochemistry of gas–phase reactions of CF3CHFCF2OCF3 with OH radicals and Cl atoms and fate of alkoxy radical at 298 K

ARTICLE *in* JOURNAL OF FLUORINE CHEMISTRY · OCTOBER 2014

Impact Factor: 1.95 · DOI: 10.1016/j.jfluchem.2014.08.001

4 AUTHORS:

Dr. Nand Kishor Gour

Tezpur University

12 PUBLICATIONS **39** CITATIONS

SEE PROFILE

Ramesh Chandra

Indian Institute of Technology Roorkee

186 PUBLICATIONS **1,530** CITATIONS

SEE PROFILE

Hari Singh

Deen Dayal Upadhyaya Gorakhpur University

51 PUBLICATIONS **402** CITATIONS

SEE PROFILE

Bhupesh Kumar Mishra

D. N. Government College, Itanagar, Arunac…

45 PUBLICATIONS **279** CITATIONS

SEE PROFILE

Journal of Fluorine Chemistry 166 (2014) 110–116

Contents lists available at ScienceDirect

Journal of Fluorine Chemistry

journal homepage: www.elsevier.com/locate/fluor

Theoretical studies on kinetics, mechanism and thermochemistry of gas-phase reactions of $CF_3CHFCF_2OCF_3$ with OH radicals and Cl atoms and fate of alkoxy radical at 298 K

Nand Kishor Gour [a], Ramesh Chandra Deka [b], Hari Ji Singh [a], Bhupesh Kumar Mishra [b,*]

[a] Department of Chemistry, D.D.U. Gorakhpur University, Gorakhpur 273009, Uttar Pradesh, India
[b] Department of Chemical Sciences, Tezpur University, Napaam, Tezpur 784 028, Assam, India

ARTICLE INFO

Article history:
Received 2 April 2014
Received in revised form 28 July 2014
Accepted 3 August 2014
Available online 12 August 2014

Keywords:
Hydrogen abstraction
Isodesmic reactions
Bond dissociation energy
Atmospheric lifetime
Hydrofluorocarbon radical decomposition

ABSTRACT

Detailed theoretical investigation has been performed on the mechanism, kinetics and thermochemistry of the gas phase reactions of $CF_3CHFCF_2OCF_3$ with OH radicals and Cl atoms using M06-2X/6-31+G(d,p) level of theory. The energetic calculations were refined by using aug-cc-pVTZ basis set. Our calculations reveal that OH-initiated hydrogen abstraction is thermodynamically and kinetically more facile than that from the Cl-initiated hydrogen abstraction. Using group-balanced isodesmic reactions, the standard enthalpies of formation (ΔH_f°) for species and bond dissociation energies for C–H bond are also reported. The ΔH_f° for $CF_3CHFCF_2OCF_3$ and $\bullet CF(CF_3)CF_2OCF_3$ species calculated from M06-2X/6-31+G(d,p) results are −523.15 and −471.65 kcal mol^{-1}, respectively. The rate constants evaluated by canonical transition state theory (CTST) are found to be 1.22×10^{-15} and 3.40×10^{-17} cm^3 $molecule^{-1}$ s^{-1} which are in a reasonable agreement with the available experimental data of $(1.43 \pm 0.28) \times 10^{-15}$ and $(4.09 \pm 0.42) \times 10^{-17}$ cm^3 $molecule^{-1}$ s^{-1}, respectively, for OH and Cl-initiated hydrogen abstraction reactions. The atmospheric life time of $CF_3CHFCF_2OCF_3$ is estimated to be 38.5 years. The atmospheric fate of the alkoxy radical, $CF_3CF(O\bullet)CF_2OCF_3$ is also investigated for the first time using same level of theory.

1. Introduction

Recently, volatile organic compounds like hydrofluoroethers (HFEs) are designed and widely recommended as a third generation replacement for chlorofluorocarbons (CFCs), hydrofluorocarbons (HFCs) and hydrochlorofluorocarbons (HCFCs) in applications such as cleaning of electronic equipment, heat transfer fluids in refrigerators, lubricant deposition and foam blowing agents [1–4]. Hydrofluoroethers do not contain chlorine and bromine atoms that cause ozone depletion [5]. In addition the rate constant for the reaction of HFEs with OH radicals suggest that their atmospheric lifetime should be relatively short and thus HFEs appear to have less impact for global warming [6]. Like most volatile organic compounds, HFEs containing C–H bonds are removed from the troposphere by reactions with atmospheric oxidants, OH radicals being the most dominant oxidant [7]. Although global atmospheric abundance of OH radicals is around 2 orders of magnitude greater than that of chlorine atoms, Cl reactions are generally faster than OH reactions, so their contribution to the degradation of VOCs may not be negligible compared to the role of OH radicals [8]. This contribution of Cl could be significant in areas where the concentration of Cl precursor species has been reported to be high, such as the coastal boundary layer [9]. Thus, chlorine atom also plays an important role in atmospheric chemistry [10]. The tropospheric oxidation of HFEs (containing $-CH_2$ group in alpha position) is known to produce the corresponding fluorinated esters (FESs) [11,12]. The degradation of FESs produces trifluoroacetic acid (TFA) which is classified as detrimental to aquatic life [13]. Hence it is important to study the kinetics and mechanistic degradation pathways of HFEs in the troposphere for complete assessment of its atmospheric chemistry as well as its impact on global warming and climate change. Considerable attention has been paid in recent years to performing experimental and theoretical studies on the reactivity of HFEs with OH radicals and Cl atoms [14–26]. $CF_3CHFCF_2OCF_3$ has been used as a fire extinguishing agent and thus may be released into the atmosphere during its use. Prior to its industrial use, appraisal of the environmental impact of $CF_3CHFCF_2OCF_3$ is needed. This motivated us to perform a

* Corresponding author. Tel.: +91 9706362213; fax: +91 3712267005.
E-mail addresses: bhupesh@tezu.ernet.in, bhupesh_chem@rediffmail.com (B.K. Mishra).

http://dx.doi.org/10.1016/j.jfluchem.2014.08.001
0022-1139/

comprehensive study on sound theoretical basis. In the present work, we have studied the mechanism and kinetics of OH and Cl-initiated H-abstraction reactions from $CF_3CHFCF_2OCF_3$ using DFT methods. Our calculation suggests that a reaction channel is feasible for the $CF_3CHFCF_2OCF_3$ + OH/Cl reactions as given below.

$$CF_3CHFCF_2OCF_3 + \bullet OH \rightarrow \bullet CF(CF_3)CF_2OCF_3 + H_2O \quad (R1)$$

$$CF_3CHFCF_2OCF_3 + \bullet Cl \rightarrow \bullet CF(CF_3)CF_2OCF_3 + HCl \quad (R2)$$

Two experimental studies were reported for reactions (R1) and (R2) by Wallington et al. [14] and Wilson et al. [15]. Wallington et al. [14] first studied the hydrogen abstraction channel of these reactions using Fourier transform infrared (FTIR) smog chamber techniques in 700 Torr of N_2/O_2 diluent at 296 K and the experimental rate constant were reported as $k_{OH} = (1.43 \pm 0.28) \times 10^{-15}$ and $k_{Cl} = (4.09 \pm 0.42) \times 10^{-17}$ cm^3 $molecule^{-1}$ s^{-1}. Subsequently, Wilson et al. [15] performed another experimental study by using relative rate methods and they also reported a rate constants value as $k(OH + CF_3CHFCF_2OCF_3) = 1.84 \times 10^{-15}$ cm^3 $molecule^{-1}$ s^{-1} at 298 K. Moreover, experimental study provides only the total rate constant and it is difficult to predict the detailed mechanism and thermochemistry. Thus, for better understanding of mechanistic pathways, kinetics and thermochemistry we must rely on quantum chemical methods. To the best of our knowledge, this is the first detailed theoretical study on gas-phase reactions with OH radicals and Cl atoms of this hydrofluoroethers. Bond dissociation energies (BDEs) of the breaking C–H bonds are known to be strongly correlated with the observed reactivity trend for the hydrogen abstraction reactions from hydrofluoroethers. Thus, we also estimated BDE of C–H bond in $CF_3CHFCF_2OCF_3$. However, no theoretical or experimental study on standard enthalpy of formation has been reported so far for these species. Here, we predict the enthalpies of formation using isodesmic reactions at M06-2X/6-31+G(d,p) level. In order to have reliable thermochemical properties and the barrier heights for reaction channels (R1) and (R2), single point energy calculations were also performed at the M06-2X/aug-cc-pVTZ level.

2. Results and discussion

2.1. Structure and energetics

The calculated enthalpy of reaction (ΔH_r°) and free energy of reaction (ΔG_r°) at 298 K for the reactions of $CF_3CHFCF_2OCF_3$ with OH radicals and Cl atoms are recorded in Table 1. The enthalpy of reaction, (ΔH_r°) values given in Table 1 shows that reaction (R1) is significantly exothermic and thus thermodynamically more facile. One transition state (TS) is located for each of the two reactions $CF_3CHFCF_2OCF_3$ + •OH and $CF_3CHFCF_2OCF_3$ + •Cl.

In the entrance channel for reaction (R1), pre- reactive complex (COMR1) has been located in the present work. In the exit channel, there is also product complex occurring before the release of the final products, which are labeled as COMP1. In pre-reactive complex (COMR1), OH radical interacts with $CF_3CHFCF_2OCF_3$ compound. The interatomic distances between the H-atom of OH radical and the O-atom of the $CF_3CHFCF_2OCF_3$ are found to be 2.315 and 2.704 Å, respectively, while the other bond lengths are very close to those in equilibrium structures. At the same time, the post-reaction complex (COMP1) with energy less than the corresponding products are located at the exits of the reaction channel (R1) for reactions with OH radicals as shown in Fig. 1. So it is clear that the reaction channel (R1) may proceed via indirect mechanisms. The indirect mechanism means reaction channel precede through reactants ≥ reactant complex ≥ TS ≥ product complex ≥ products. The search of stationary points was made along the minimum energy path on a relaxed potential energy surface. Optimized geometries of reactants, reactant complex, transition states, product complex and products obtained at the M06-2X/6-31+G(d,p) level are shown in Fig. 1.

Table 1
Reaction enthalpies, free energies of reactions, free energies of activation and bond dissociation energy calculated at M06-2X/6-31+G(d,p) and M06-2X/aug-cc-pVTZ levels of theory. All values are in kcal mol^{-1}.

	M06-2X/6-31+G(d,p)	M06-2X/aug-cc-pVTZ
ΔH_r°		
Reaction (R1)	−15.23	−13.58
Reaction (R2)	−0.03	2.75
Reaction (R6)	3.05	−1.06
Reaction (R7)	5.48	2.65
ΔG_r°		
Reaction (R1)	−16.37	−14.69
Reaction (R2)	−2.37	0.41
Reaction (R6)	−11.41	−14.54
Reaction (R7)	−8.54	−11.37
$\Delta G^\#$		
Reaction (R1)	12.48	12.26
Reaction (R2)	14.93	14.13
Reaction (R6)	10.24	9.86
Reaction (R7)	13.61	13.10
D°		
$CF_3C^*HFCF_2OCF_3$	103.64	105.29

During the formation of transition states, important structural parameters that have to be observed are the C–H bond of the leaving hydrogen and the newly formed bond between H and O atom in the OH radical. Visualization of the optimized structure of TS1 further reveals that the breaking C–H (C2–H1) bond is found to be longer by 11.70% than the observed C–H bond length in isolated $CF_3CHFCF_2OCF_3$ molecule whereas the forming O...H bond length is longer by 33.37% than the O–H bond length in H_2O. The fact that the elongation of forming bond is larger than that of the breaking bond indicates that the barrier of the reaction (R1) is near the corresponding reactants. This means the reaction (R1) will precede via early transition state structure which is consistent with Hammond's postulate [27] applied to an exothermic hydrogen abstraction reaction. Similarly, for transition state TS2 for reaction (R2), the length of the breaking C–H (C2–H1) bond is found to be longer by 31.44% than the observed C–H bond length in isolated $CF_3CHFCF_2OCF_3$ molecule whereas the forming H···Cl (H1–Cl1) bond length is longer by 11.56% than the H–Cl bond length in isolated HCl molecule. This implies that the barrier of the reaction (R2) is closer to the products, and that the reaction with Cl atoms proceeds via a late transition state.

Results obtained by frequency calculations for species involved in reactions (R1) and (R2) are recorded in Table S1 of Supporting information. These results show that the reactants, reactant complex, product complex and products have stable minima on their potential energy surface characterized by the occurrence of only real positive vibrational frequencies. On the other hand, transition states are characterized by the occurrence of only one imaginary frequency obtained at 1667*i* and 904*i* cm^{-1}, respectively, for TS1 and TS2. Visualization of the normal-mode corresponding to the calculated imaginary frequency shows a well defined transition state geometry connecting reactants and products during transition. The existence of transition state on the potential energy surface is further ascertained by intrinsic reaction coordinate (IRC) calculation [28] performed at the same level of theory. The relative energies (including ZPE) for all the species involved in reaction channels (R1) and (R2) obtained at both M06-2X/6-31+G(d,p) and M06-2X/aug-cc-pVTZ levels are given in Table S2 of Supporting information. From Table S2 of Supporting information it can be seen that the calculated barrier heights at both levels are consistent with each other. These results reveal that energy barriers for H atom abstraction by OH radicals and Cl atoms are 3.81 and 5.61 kcal mol^{-1}, respectively, at M06-2X/6-31+G(d,p) level of theory. On the other hand, the same are found to be 3.60 and 7.18 kcal mol^{-1}, respectively, at M06-2X/aug-cc-pVTZ level of

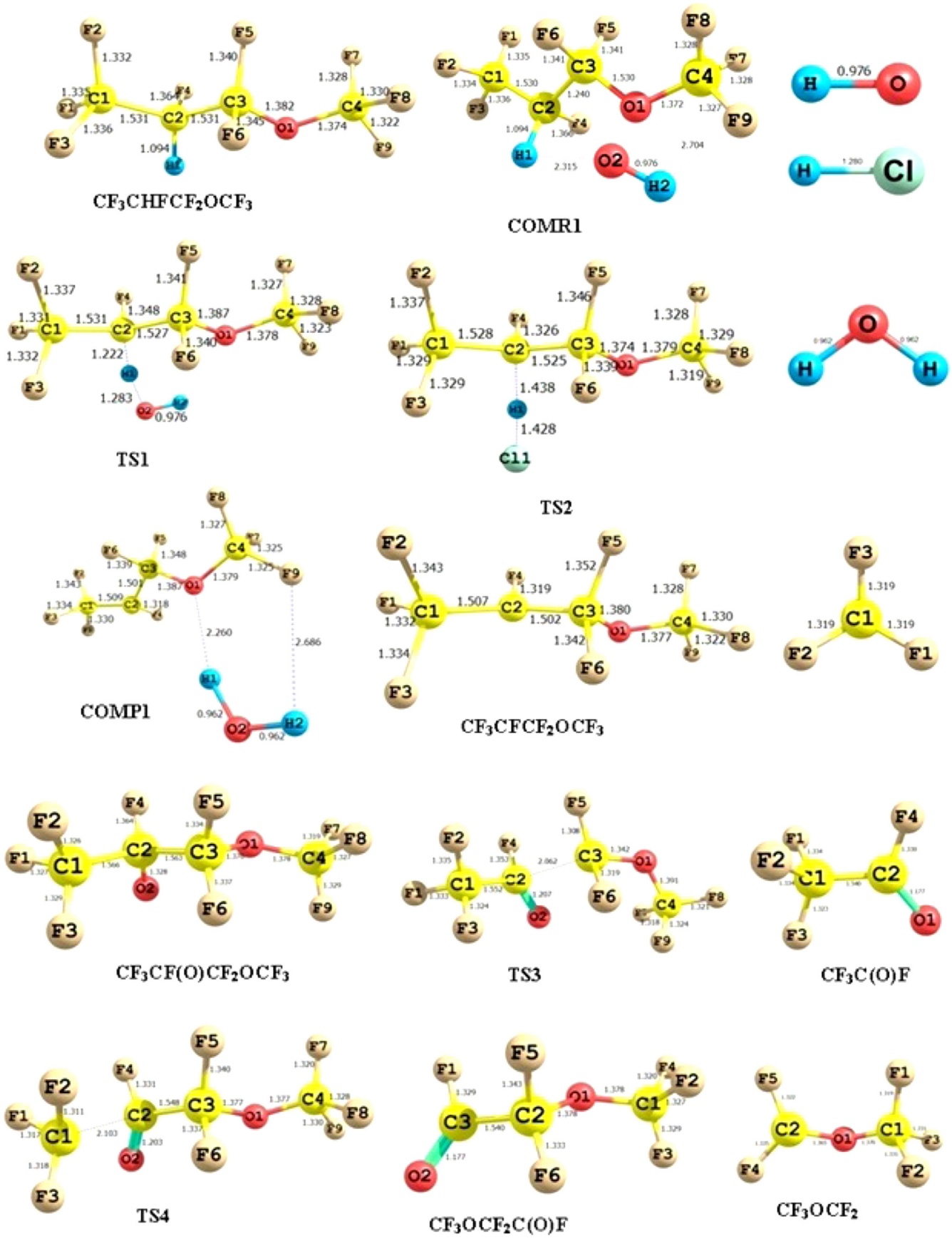

Fig. 1. Optimized geometries of reactants, reactant complex, transition states, product complex and products at M06-2X/6-31+G(d,p) level. Bond lengths are in Angstroms.

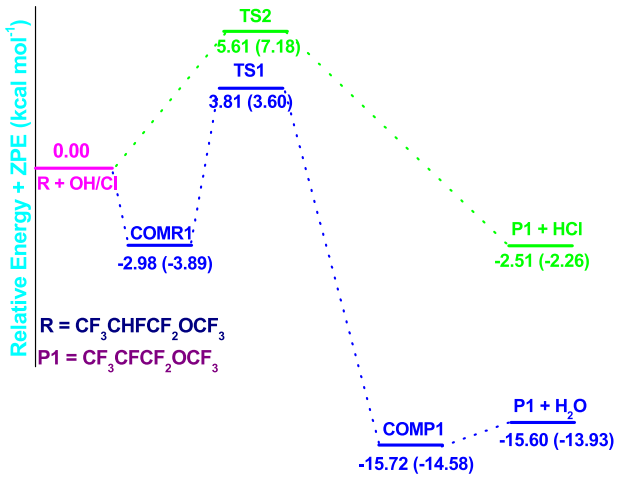

Fig. 2. Schematic potential energy diagram for the $CF_3CHFCF_2OCF_3$ + OH/Cl reactions. Relative energies (in kcal mol^{-1}) with ZPE at M06-2X/aug-cc-pVTZ level. The values given in parentheses are calculated at M06-2X/6-31+G(d,p) + ZPE level of theory.

theory. The barrier height values suggest that H-abstraction by OH radicals is kinetically more favorable than that by Cl atoms. A potential energy diagram of the title reaction is constructed and shown in Fig. 2. In the construction of energy diagram, zero-point energy corrected total energy data as recorded in Table S2 of Supporting information are utilized. Total energy (including zero-point energy) for all the species is determined with respect to the reactants ($CF_3CHFCF_2OCF_3$ + OH/Cl) setting it arbitrarily at zero. The values given in parentheses in Fig. 2 are ZPE corrected values obtained at M06-2X/6-31+G(d,p) level. Moreover, spin contamination is not important for the $CF_3CHFCF_2OCF_3$ + OH/Cl reactions because $\langle S^2 \rangle$ is found to be 0.76 at M06-2X/6-31+G(d,p) before annihilation that is only slightly larger than the expected value of $\langle S^2 \rangle$ = 0.75 for doublets.

The group-balanced isodesmic reactions, in which the number and types of bonds are conserved, are used as working chemical reactions herein to calculate the ΔH_f°. Here, three isodesmic reactions are used to estimate the enthalpies of formation of $CF_3CHFCF_2OCF_3$. The isodesmic reactions used are as follows:

$$CF_3CHFCF_2OCF_3 + CH_2F_2 \rightarrow CF_3CH_2OCHF_2 + CF_3CF_3 \quad (R3)$$

$$CF_3CHFCF_2OCF_3 + CH_4 \rightarrow CF_3CF_2CH_2OCH_3 + CF_4 \quad (R4)$$

$$CF_3CHFCF_2OCF_3 + CH_3F \rightarrow CF_3CHFOCH_3 + CF_3CF_3 \quad (R5)$$

All geometrical parameters of the species involved in the isodesmic reactions (R3)–(R5) were first optimized at the M06-2X/6-31+G(d,p) level and then energies of the species were further refined at M06-2X/aug-cc-pVTZ level of theory. At first we have calculated the reaction enthalpies (ΔH_r°) of the isodesmic reactions (R3)–(R5) as mentioned above using total energies of the species obtained at M06-2X/aug-cc-pVTZ level including thermal correction to enthalpy estimated at M06-2X/6-31+G(d,p) level. Since, the (ΔH_r°) value corresponds to the difference of the enthalpy of formation (ΔH_f°) values between the products and the reactants, the (ΔH_f°) values of the reactant and product species are easily evaluated by combining them with the known enthalpies of formation of the reference compounds involved in our isodesmic reaction schemes. The experimental ΔH_f° values for CH_2F_2: −107.77 kcal mol^{-1} [29], $CF_3CH_2OCHF_2$: −319.07 kcal mol^{-1} [30] $CF_3CHFOCH_3$: −257.23 kcal mol^{-1} [31], CF_3CF_3: −320.89 kcal mol^{-1} [31] CH_3F: −56.8 kcal mol^{-1} [31], CH_4: −17.9 kcal mol^{-1} [32] CF_4: −223.08 kcal mol^{-1} [29], and $CF_3CF_2CH_2OCH_3$: −309.99 kcal mol^{-1} [30] were thus used to evaluate the required enthalpies of formation. The calculated values of enthalpies of formation are listed in Table 2. As can be seen from Table 2, the values of ΔH_f° for the species obtained by the three working chemical reactions at both levels are consistent with each other. The average ΔH_f° for $CF_3CHFCF_2OCF_3$ calculated from M06-2X/6-31+G(d,p) and M06-2X/aug-cc-pVTZ results are −523.15 and −522.61 kcal mol^{-1}, respectively. The ΔH_f° value for $\bullet CF(CF_3)CF_2OCF_3$ radical can also be easily calculated from the reported ΔH_r° value for reaction (R1) in Table 1, the calculated ΔH_f° value for $CF_3CHFCF_2OCF_3$ and the experimental ΔH_f° values for H_2O (−57.8 kcal mol^{-1}) and •OH (8.93 kcal mol^{-1}) radical [33]. The ΔH_f° values for $\bullet CF(CF_3)CF_2OCF_3$ radical calculated from the M06-2X/6-31+G(d,p) and M06-2X/aug-cc-pVTZ results are found to be −471.65 and −469.46 kcal mol^{-1}, respectively. Although no comparison between theory and experiment can be made due to the lack of the experimental data, the heat of formation (ΔH_f°) values can be expected to provide good reference information for upcoming laboratory investigations. The calculated bond-dissociation energies, BDE (D°) of the C–H bond of $CF_3CHFCF_2OCF_3$ molecule obtained from the M06-2X/6-31+G(d,p) and M06-2X/aug-cc-pVTZ results amount to be 103.64 and 105.29 kcal mol^{-1}, respectively. No comparison between theory and experiment can be made due to the lack of the experimental D° values. Moreover, our calculated BDE values for the C–H bond is found to be in reasonable agreement with the theoretical value of 101.04 and 100.66 kcal mol^{-1}, respectively, for –CHF and $-CH_3$ sites of $CF_3CHFCF_2OCH_3$ reported by Urata et al. [16] using artificial neural network (ANN) technique. Our calculated BDE for –CHF site is found to be somewhat higher than the corresponding values for $CF_3CHFCF_2OCH_3$ molecule. This is in line of the fact that fluorine atom substitution for hydrogen atom on carbon atom reduces the reactivity of the C–H bond toward hydrogen abstraction.

Table 2
Enthalpies of formation (ΔH_f°) for the species at 298 K from the isodesmic reactions. All values are in kcal mol^{-1}.

Species	Reaction schemes	M06-2X/ 6-31+G(d,p)	M06-2X/ aug-cc-pVTZ
$CF_3CHFCF_2OCF_3$	(R3)	−523.14	−522.90
	(R4)	−523.30	−522.64
	(R5)	−523.01	−522.30
Average		−523.15	−522.61
$\bullet CF(CF_3)CF_2OCF_3$		−471.65	−469.46

2.2. Rate constant calculation

At 298 K, our calculated k_{OH} value using M06-2X/6-31+G(d,p) barrier height is found to be 1.22×10^{-15} which is in a reasonable agreement with the experimental value of $(1.43 \pm 0.28) \times 10^{-15}$ cm^3 $molecule^{-1}$ s^{-1} reported by Wallington et al. [14] and 1.84×10^{-15} cm^3 $molecule^{-1}$ s^{-1} by Wilson et al. [15]. However, the rate coefficient obtained from the M06-2X/aug-cc-pVTZ result (0.90×10^{-15} cm^3 $molecule^{-1}$ s^{-1}) is also in a reasonable agreement with the M06-2X/6-31+G(d,p) and experimental values at 298 K. Similarly, the rate constant for H atom abstraction reaction of $CF_3CHFCF_2OCF_3$ by Cl atoms as given by reaction (R2) is calculated as $k_{Cl} = 3.40 \times 10^{-17}$ cm^3 $molecule^{-1}$ s^{-1} and 2.41×10^{-17} cm^3 $molecule^{-1}$ s^{-1} at 298 K using M06-2X/6-31+G(d,p) and M06-2X/aug-cc-pVTZ barrier heights, respectively, which are in a reasonable agreement with experimental value of $(4.09 \pm 0.42) \times 10^{-17}$ cm^3 $molecule^{-1}$ s^{-1} reported by Wallington et al. [14]. From our theoretical study it can be concluded that OH-initiated H-abstraction of $CF_3CHFCF_2OCF_3$ is more facile as compared to its Cl-initiated H-abstraction reactions.

2.3. Atmospheric implications

The lifetime of HFEs in the atmosphere is thought to depend almost completely on reaction with hydroxyl radicals. In general, tropospheric lifetime (τ_{eff}) of $CF_3CHFCF_2OCF_3$ can be estimated by assuming that its removal from troposphere occurs mainly through the reactions with OH radicals. Then (τ_{eff}) can be expressed as [34]

$$\tau_{eff} \approx \tau_{OH}$$

However, this equation does not take into consideration the errors due to the vertical temperature profile of the troposphere. When calculating OH-based lifetimes, the use of 272 K as an average tropospheric temperature and methyl chloroform (CH_3CCl_3), as a chemical of well known source and sink, has been suggested [35] to minimize the errors resulting from neglecting the specific temperature dependences. Thus, lifetime estimations for HFEs are generally calculated on the basis of gas-phase removal by OH only and with methyl chloroform (MCF) as reference:

$$\tau_{OH}^{HFE} = \frac{k_{MCF}(272\,K)}{k_{HFE}(272\,K)}\tau_{OH}^{MCF}$$

where τ_{OH}^{HFE} is the lifetime for $CF_3CHFCF_2OCF_3$, k_{HFE} and k_{MCF} are the rate constants for the reactions of OH radicals with $CF_3CHFCF_2OCF_3$ and methyl chloroform (MCF), respectively, at $T = 272$ K and $\tau_{OH}^{MCF} = 5.99$ years [35]. Taking the values of rate constants for $k_{MCF} = 6.14 \times 10^{-15}$ from Ref. [35] and calculated rate constant of $CF_3CHFCF_2OCF_3$ $k_{HFE} = 0.95 \times 10^{-15}$ cm^3 $molecule^{-1}$ s^{-1}, at 272 K, the estimated lifetime is found to be 38.5 years which is in good agreement with the reported value of 40.0 years [14,36].

2.4. Atmospheric fate of alkoxy radical

A general mechanism of tropospheric degradation of $CF_3CHFCF_2OCF_3$ is shown in Scheme 1. The tropospheric degradation of $CF_3CHFCF_2OCF_3$ is initiated by attack of OH radicals or Cl atoms which leads to the formation of haloalkyl radical $\bullet CF(CF_3)CF_2OCF_3$. The latter reacts with atmospheric O_2 to produce peroxy radical, $CF_3CF(OO\bullet)CF_2OCF_3$. In a polluted atmosphere the peroxy radical react with other oxidizing species such as NO_2 and NO that ultimately leads to the formation of alkoxy radical $CF_3CF(O\bullet)CF_2OCF_3$. The chemistry of alkoxy radicals has been a subject of extensive experimental and theoretical investigations as these species are key intermediates in the atmospheric oxidation of halogenated hydrocarbons [37–43].

Due to the significant role played by alkoxy radicals formed in the destruction of a variety of organic compounds released into the atmosphere, studying the fate of $CF_3CF(O\bullet)CF_2OCF_3$ is needed from the viewpoint of understanding its role in the atmospheric chemistry. To the best of our knowledge, no theoretical study has been performed to elucidate the dissociative pathways of $CF_3CF(O\bullet)CF_2OCF_3$ radical. The fate of fluoroalkoxy radical $CF_3CF(O\bullet)CF_2OCF_3$ produced during its thermal decomposition in the atmosphere is envisaged to occur via the following reactions:

$$CF_3CF(O\bullet)CF_2OCF_3 \rightarrow CF_3C(O)F + \bullet CF_2OCF_3 \quad (R6)$$

$$CF_3CF(O\bullet)CF_2OCF_3 \rightarrow \bullet CF_3 + CF_3OCF_2C(O)F \quad (R7)$$

The detailed thermodynamic calculations performed at M06-2X/6-31+G(d,p) and M06-2X/aug-cc-pVTZ levels for reaction enthalpies and free energies associated with reaction channels (R6) and (R7) are listed in Table 1. Free energy values show that both reactions are exergonic ($\Delta G_r^\circ < 0$). The results given in Table 1 reveal that both the reaction channels are thermodynamically facile, but reaction channels (R6) is more favorable than that of reaction channel (R7). Optimized geometries of radical, transition states and products obtained at the M06-2X/6-31+G(d,p) level are shown in Fig. 1. Transition states obtained on the potential energy surfaces of reactions (R6) and (R7) are characterized as TS3 and TS4, respectively. In the optimized structure of TS3 the elongation of the C–C bond (C2–C3) is found to be 1.563 to 2.062 Å (about 32% increases) with a simultaneous shrinkage of the C2–O2 bond. This decrease has been found to be almost 9% (1.328 to 1.207 Å). Similar analysis made on the optimized structure of TS4 reveals the elongation of C2–C3 bond length from 1.566 to 2.103 Å resulting in an increase of about 34% accompanied with a shrinkage of the C–O bond (C2–O2) 1.328 to 1.203 (~9%). Harmonic vibrational frequencies for reactant, transition states and products involved in reactions (R6) and (R7) are recorded in Table S1 of Supporting information. These results show that transition states are characterized by the occurrence of only one imaginary frequency obtained at 283*i* and 317*i* cm^{-1} for TS3 and TS4, respectively. Visualization of the listed imaginary frequencies gives a qualitative conformation of

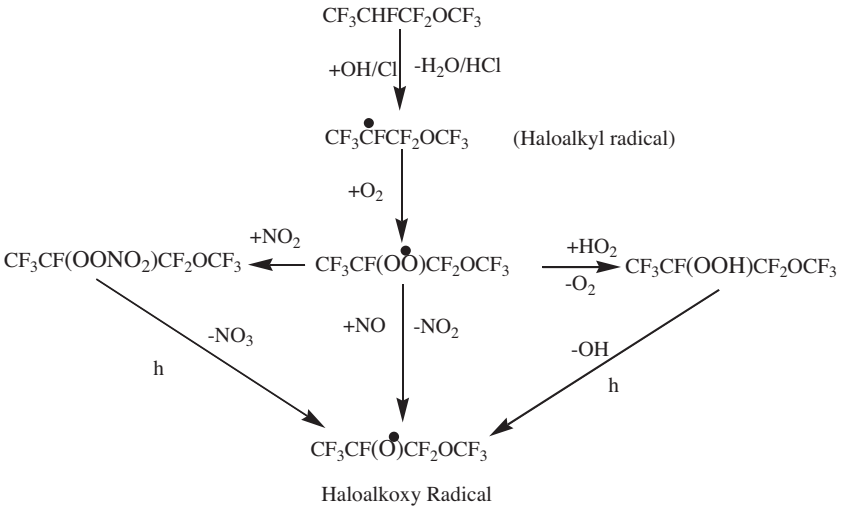

Scheme 1. Tropospheric degradation of CF3CHFCF2OCF3.

the existence of transition states connecting reactant and products. The existence of the correct transition state on the potential energy surface, however, is ascertained by intrinsic reaction coordinate (IRC) calculation [28] performed at the same level of theory. The associated energy barriers corresponding to reactions (R6) and (R7) are recorded in Table S2 of Supporting information. Results show that the M06-2X/aug-cc-pVTZ method yields a value of 9.21 and 10.31 kcal mol^{-1} for TS3 and TS4, respectively. On the other hand, the M06-2X/6-31+G(d,p) method yields corresponding values as 11.38 and 12.82 kcal mol^{-1}. No experimental or theoretical data are available in the literature to compare the energy barriers associated with the decomposition channels of $CF_3CF(O\bullet)CF_2OCF_3$ radical considered during the present investigation. Thus, we conclude that the atmospheric fate of $CF_3CF(O\bullet)CF_2OCF_3$ radical is C–C bond scission leading to the formation of $CF_3C(O)F$ and $\bullet CF_2OCF_3$ radical. Our result agrees well with the experimental observation of near-unity production of $CF_3C(O)F$ made by Wallington et al. [14] indicating that (R6) is dominating fate of this radical. $CF_3C(O)F$ produced in reaction (R6) undergoes hydrolysis to give HF and trifluoroacetic acid (TFA).

3. Conclusions

The potential energy surface and reaction kinetics of the H atom abstraction reaction of $CF_3CHFCF_2OCF_3$ with OH radicals and Cl atoms are investigated at M06-2X/6-31+G(d,p) level of theory. The reaction with OH radicals is found to follow an indirect path through the formation of pre- and post- reaction complexes. The barrier height for hydrogen abstraction by OH radicals and Cl atoms are found to be 3.81 and 5.61 kcal mol^{-1}, respectively. The thermal rate constant for the H atom abstraction of $CF_3CHFCF_2OCF_3$ by OH radicals and Cl atoms are found to be 1.22×10^{-15} and 3.40×10^{-17} cm^3 $molecule^{-1}$ s^{-1} at 298 K using canonical transition state theory which are in good agreement with experimental data. From our theoretical study it can be concluded that OH-initiated hydrogen abstraction is thermodynamically and kinetically more facile than that of Cl-initiation. The ΔH_f° for $CF_3CHFCF_2OCF_3$ and $\bullet CF(CF_3)CF_2OCF_3$ species calculated from M06-2X/6-31+G(d,p) results are −523.15 and −471.65 kcal mol^{-1}, respectively. The D° value obtained for the C–H bond of $CF_3CHFCF_2OCF_3$ amount to 103.64 kcal mol^{-1}. Atmospheric lifetime of $CF_3CHFCF_2OCF_3$ is estimated to be 38.5 years. These data can be useful for further thermo-kinetic modeling of other reactions involving these species. The unimolecular decomposition reactions of the alkoxy radical, $CF_3CF(O\bullet)CF_2OCF_3$ at M06-2X level is also explored. Our results reveal that the sole atmospheric fate for thermal decomposition of $CF_3CF(O\bullet)CF_2OCF_3$ radical is the C–C bond scission that occurs with the lowest barrier height.

4. Computational methods

Geometry optimization of the species were made at the M06-2X [44] level of theory using 6-31+G(d,p) basis set. The 6-31+G(d,p) was chosen because the same basis set was used for developing the model functional. Previous works have shown that the M06-2X hybrid density functional provides reliable results for thermochemistry and kinetics [45–50]. The M06-2X is a hybrid meta-DFT method with a high percentage of HF exchange, and it has broadest applicability with average mean absolute errors of about 1.3, 1.2, and 0.5 kcal mol^{-1}, respectively, for thermochemical, barrier height and non-covalent interaction calculations [51]. Since the formation of pre- and post-reaction complexes modifies the shape of potential energy surface for the hydrogen abstraction reactions by OH radicals and hence affects the tunneling factor [20–22,52]. As a result the rate constant for hydrogen abstraction also changes. Thus we also validated pre- and post-reactive complexes along the entry and exit of the reaction path. In order to determine the nature of different stationary points on the potential energy surface, vibrational frequencies calculations were performed using the same level of theory at which the optimization was made. Further, to ascertain that the identified transition states connect reactant and products smoothly, intrinsic reaction coordinate (IRC) calculations [28] were also performed at the M06-2X/6-31+G(d,p) level. Single point energy calculations were performed at M06-2X using aug-cc-pVTZ basis set.

The rate constant for title reactions are calculated by using canonical transition state theory [53] given by the following expression:

$$k = \sigma\kappa(T)\frac{k_B T}{h}\frac{Q_{TS}}{Q_A \times Q_B}\exp\frac{-\Delta E}{RT} \quad (1)$$

where σ is the reaction path degeneracy, $\kappa(T)$ is the tunneling correction factor at temperature T. Q_{TS}, Q_A and Q_B are the total partition functions (per unit volume) for the transition states and reactants, respectively. $\Delta E^{\#}$ is the barrier height including zero point energy correction, k_B is the Boltzmann constant, h is the Planck's constant and R represents the universal gas constant. The tunneling correction factor $\kappa(T)$ is defined as the ratio of the quantum mechanical to the classical mechanical barrier crossing rate. The tunneling correction $\kappa(T)$ was estimated by using the Eckart's unsymmetric barrier method [54,55]. In this method, the reaction path through TS is fitted first in a model potential function.

$$V = -\frac{Ay}{1-y} - \frac{By}{(1-Y)^2} \quad (2)$$

where $y = -\exp(2\pi x/L)$ and x is the variable measured along the reaction coordinate and L is the characteristic length. A and B are related to the forward and reverse energy barriers and L to the second derivative of V at its maximum written as F^* and these are given as

$$A = V_F - V_R$$
$$B = \left(\sqrt{V_F} + \sqrt{V_R}\right)^2$$
$$L = 2\pi\left(\frac{-2}{F_*}\right)^{1/2}\left(V_F^{-1/2} + V_R^{-1/2}\right)^{-1}$$

All vibrational modes, except for the lowest vibrational mode, were treated quantum mechanically as separable harmonic oscillators, whereas for the lowest-frequency mode, the partition function was evaluated by the hindered-rotor approximation by Chuang and Truhlar [56] method. Using Truhlar's procedure [57] the q^{HIN}/q^{HO} ratio was found to be close to unity. In the calculation of reactant electronic partition function, the excited state of the OH radicals is included, with a 140 cm^{-1} splitting: the $^2P_{3/2}$ and $^2P_{1/2}$ electronic states of Cl atoms are also included with 881 cm^{-1} splitting due to spin–orbit coupling. As discussed before, the H-abstraction by OH radicals proceeds via two step mechanism. The first step involves a fast pre-equilibrium (K_{eq}) between the reactants and reaction complex (RC) and the second step is the hydrogen abstraction with the rate constant $k_2^\dagger$. The overall rate constant including equilibrium constant (K_{eq}) and rate constant ($k_2^\dagger$) are given by,

$$K_{eq} = \frac{Q_{RC}}{Q_A \times Q_B}e^{(E_R - E_{RC})/RT} \quad (3)$$

and $k_2^\dagger$ can be obtained from *TST* in the from

$$k_2^\dagger = \sigma\kappa(T)\frac{k_B T}{h}\frac{Q_{TS}}{Q_{RC}}e^{-(E_{TS} - E_{RC})/RT} \quad (4)$$

The rate constant for H-abstraction from $CF_3CHFCF_2OCF_3$ via reaction (R1) is then obtained by the following expression,

$$k = K_{eq} \times k_2^{\dagger} = \sigma\kappa(T)\frac{k_B T}{h}\frac{Q_{TS}}{Q_A \times Q_B}e^{-(E_{TS}-E_R)/RT} \quad (5)$$

where Q_A, Q_B, Q_{RC} and Q_{TS} represents the total partition functions (per unit volume) of the reactants, reaction complex and transition states, respectively. E_{TS}, E_{RC} and E_R are the total energies (ZPE corrected) of transition state, reaction complex and reactants, respectively. Thus, it seems that the final expression (Eq. (5)) for estimating rate constant and barrier height turns out to be the usual CTST expression (Eq. (1)) used for the determination of rate constant and barrier height of a direct reaction, irrespective of the energy of pre-reactive hydrogen bonded complex (COMR1). However, the tunneling factor κ(T) will obviously be different due to pre- and post-reaction complex formation and as a result will affect the total rate constant. All calculations were performed with the Gaussian 09 suite of program [58].

Acknowledgments

BKM is thankful to University Grants Commission, New Delhi for providing Dr. D. S. Kothari Fellowship (No. F.13-696/2012(BSR)). NKG and HJS are thankful to Council of Scientific and Industrial Research, New Delhi for providing financial assistance in form of a project (No. 01/2402/10-EMR-II). We are also thankful to the learned reviewers for their constructive suggestions to improve the quality of the manuscript.

Appendix A. Supplementary data

Supplementary data associated with this article can be found, in the online version, at http://dx.doi.org/10.1016/j.jfluchem.2014.08.001.

References

[1] W.T. Tsai, J. Hazard. Mater. 119 (2005) 69–78.
[2] A. Sekiya, S. Misaki, J. Fluorine Chem. 101 (2000) 215–221.
[3] R.L. Powell, J. Fluorine Chem. 114 (2002) 237–250.
[4] A. McCulloch, J. Fluorine Chem. 100 (1999) 163–173.
[5] R. Imasu, A. Suga, T. Matsuno, J. Meteorol. Soc. Jpn. 73 (1995) 1123–1136.
[6] P. Blowers, K.F. Tetrault, Y.T. Morehead, Theor. Chem. Acc. 119 (2008) 369–381.
[7] V.C. Papadimitriou, K.G. Kambanis, Y.G. Lazarou, P. Papagiannakopoulos, J. Phys. Chem. A 108 (2004) 2666–2674.
[8] Y.D. Mera, A. Aranda, I. Bravo, E. Moreno, E. Martinez, A. Rodriguez, Chem. Phys. Lett. 479 (2009) 20–24.
[9] G.C. Tiu, Fu-Ming Tao, Chem. Phys. Lett. 428 (2006) 42–48.
[10] W. Zierkiewicz, Chem. Phys. Lett. 555 (2013) 72–78.
[11] I. Bravo, Y. Díaz-de-Mera, A. Aranda, E. Moreno, D.R. Nutt, G. Marston, Phys. Chem. Chem. Phys. 13 (2011) 17185–17193.
[12] N. Oyaro, S.R. Sellevag, C.J. Neilsen, Environ. Sci. Technol. 38 (2004) 5567–5576.
[13] A. Jordan, H. Frank, Environ. Sci. Technol. 33 (4) (1999) 522–527.
[14] T.J. Wallington, M.D. Hurley, O.J. Nielsen, M.P. Sulbaek Andersen, J. Phys. Chem. A 108 (2004) 11333–11338.
[15] E.W.JJr. Wilson, W.A. Hamilton, H.R. Mount, W.B. DeMore, J. Phys. Chem. A 111 (2007) 1610–1617.
[16] S. Urata, A. Takada, T. Uchimaru, A.K. Chandra, Chem. Phys. Lett. 368 (2003) 215–223.
[17] K. Tokuhashi, L. Chen, S. Kutsuna, T. Uchimaru, M. Sugie, A. Sekiya, J. Fluorine Chem. 125 (2004) 1801–1807.
[18] K. Takahashi, Y. Matsumi, T.J. Wallington, M.D. Hurley, Chem. Phys. Lett. 352 (2002) 202–208.
[19] H.J. Singh, B.K. Mishra, J. Mol. Model. 16 (2010) 1473–1480.
[20] Kh.J. Devi, A.K. Chandra, Chem. Phys. Lett. 502 (2011) 23–28.
[21] H.J. Singh, B.K. Mishra, J. Mol. Model. 17 (2011) 415–422.
[22] A.K. Chandra, J. Mol. Model. 18 (2012) 4239–4247.
[23] G. Fontana, M. Causa, V. Gianotti, G. Marchionni, J. Fluorine Chem. 109 (2001) 113–121.
[24] H.J. Singh, B.K. Mishra, P.K. Rao, Bull. Korean Chem. Soc. 31 (2010) 3718–3722.
[25] M. Lily, D. Sutradhar, A.K. Chandra, Comp. Theor. Chem. 1022 (2013) 50–58.
[26] B.K. Mishra, M. Lily, A.K. Chakrabartty, R.C. Deka, A.K. Chandra, J. Fluorine Chem. 159 (2014) 57–64.
[27] G.S. Hammond, J. Am. Chem. Soc. 77 (1955) 334–338.
[28] C. Gonzalez, H.B. Schlegel, J. Chem. Phys. 90 (1989) 2154–2161.
[29] J. Csontos, Z. Rolik, S. Das, M. Kallay, J. Phys. Chem. A 114 (2010) 13093–13103.
[30] S. Kondo, A. Takahashi, K. Tokuhashi, A. Sekiya, Y. Yamada, K. Saito, J. Fluorine Chem. 117 (2002) 47–53.
[31] H. Sun, H. Gong, X. Pan, L. Hao, C. Sun, R. Wang, X. Huang, J. Phys. Chem. A 113 (2009) 5951–5957.
[32] M.W. Chase Jr., NIST-JANAF thermochemical tables, fourth edition, J. Phys. Chem. Ref. Data 9 (1998) 1–1951.
[33] D.R. Lide, CRC Handbook of Chemistry and Physics, 89th ed., CRC Press, New York, NY, 2009.
[34] M.J. Kurylo, V.L. Orkin, Chem. Rev. 103 (2003) 5049–5076.
[35] C.M. Spivakovsky, J.A. Logan, S.A. Montzka, Y.J. Balkanski, M. Foreman-Fowler, D.B.A. Jones, L.W. Horowitz, A.C. Fusco, C.A.M. Brenninkmeijer, M.J. Prather, S.C. Wofsy, M.B. McElroy, J. Geophys. Res. 105 (2000) 8931–8980.
[36] Ø. Hodnebrog, M. Etminan, J.S. Fuglestvedt, G. Marston, G. Myhre, C.J. Nielsen, K.P. Shine, T.J. Wallington, Rev. Geophys. 51 (2013) 300–378.
[37] J.J. Orlando, G.S. Tyndall, T.J. Wallington, Chem. Rev. 103 (2003) 4657–4690.
[38] L. Vereecken, J.S. Francisco, Chem. Soc. Rev. 41 (2012) 6259–6293.
[39] M.A. Ferenac, A.J. Davis, A.S. Holloway, T.S. Dibble, J. Phys. Chem. A 107 (2003) 63–72.
[40] M.T. Rayez, B. Picquet-Varrault, F. Caralpa, J.C. Rayez, Phys. Chem. Chem. Phys. 4 (2002) 5789–5794.
[41] B.K. Mishra, RSC Adv. 4 (2014) 16759–16764.
[42] H.J. Singh, B.K. Mishra, J. Chem. Sci. 123 (2011) 733–741.
[43] H.J. Singh, B.K. Mishra, N.K. Gour, Theor. Chem. Acc. 125 (2010) 57–64.
[44] Y. Zhao, D.G. Truhlar, Theor. Chem. Acc. 120 (2008) 215–241.
[45] R.C. Deka, B.K. Mishra, J. Mol. Graphics Modell. 53 (2014) 23–30.
[46] B.K. Mishra, M. Lily, A.K. Chakrabartty, D. Bhattacharjee, R.C. Deka, A.K. Chandra, New J. Chem. 38 (2014) 2813–2822.
[47] M. Lily, B.K. Mishra, A.K. Chandra, J. Fluorine Chem. 161 (2014) 51–59.
[48] N.K. Gour, R.C. Deka, H.J. Singh, B.K. Mishra, J. Fluorine Chem. 160 (2014) 64–71.
[49] T.C. Dinadayalane, G. Paytakov, J. Leszczynski, J. Mol. Model. 19 (2013) 2855–2864.
[50] L. Sandhiya, P. Kolandaivel, K. Senthilkumar, Struct. Chem. 23 (2012) 1475–1488.
[51] D. Mandal, C. Sahu, S. Bagchi, A.K. Das, J. Phys. Chem. A 117 (2013) 3739–3750.
[52] A.K. Chakrabartty, B.K. Mishra, D. Bhattacharjee, R.C. Deka, J. Fluorine Chem. 154 (2013) 60–66.
[53] K.J. Laidler, Chemical Kinetics, third ed., Pearson Education, New Delhi, 2004.
[54] R.L. Brown, J. Res. Nat. Bur. Stand. 86 (1981) 357–359.
[55] R. Xiao, M. Noerpel, H.L. Luk, Z. Wei, R. Spinney, Int. J. Quantum Chem. 114 (2014) 74–83.
[56] Y.Y. Chuang, D.G. Truhlar, J. Chem. Phys. 112 (2000) 1221–1228.
[57] D.G. Truhlar, J. Comput. Chem. 12 (1991) 266–270.
[58] M.J. Frisch, G.W. Trucks, H.B. Schlegel, G.E. Scuseria, M.A. Robb, J.R. Cheeseman, G. Scalmani, V. Barone, B. Mennucci, G.A. Petersson, H. Nakatsuji, M. Caricato, X. Li, H.P. Hratchian, A.F. Izmaylov, J. Bloino, G. Zheng, J.L. Sonnenberg, M. Hada, M. Ehara, K. Toyota, R. Fukuda, J. Hasegawa, M. Ishida, T. Nakajima, Y. Honda, O. Kitao, H. Nakai, T. Vreven, J.A.JJr. Montgomery, J.E. Peralta, F. Ogliaro, M. Bearpark, J.J. Heyd, E. Brothers, K.N. Kudin, V.N. Staroverov, R. Kobayashi, J. Normand, K. Raghavachari, A. Rendell, J.C. Burant, S.S. Iyengar, J. Tomasi, M. Cossi, N. Rega, N.J. Millam, M. Klene, J.E. Knox, J.B. Cross, V. Bakken, C. Adamo, J. Jaramillo, R. Gomperts, R.E. Stratmann, O. Yazyev, A.J. Austin, R. Cammi, C. Pomelli, J.W. Ochterski, R.L. Martin, K. Morokuma, V.G. Zakrzewski, G.A. Voth, P. Salvador, J.J. Dannenberg, S. Dapprich, A.D. Daniels, Ö. Farkas, J.B. Foresman, J.V. Ortiz, J. Cioslowski, D.J. Fox, Gaussian 09, Revision B.01, Gaussian, Inc., Wallingford, CT, 2010.